

DFT and experimental (FT-IR and FT-Raman) investigation of vibrational spectroscopy and molecular docking studies of 2-(4-oxo-3-phenethyl-3,4-dihydroquinazolin-2-ylthio)-N-(3,4,5-trimethoxyphenyl) acetamide

Adel S. El-Azab ^{a,b}, Y. Sheena Mary ^e, C. Yohannan Panicker ^{e,*}, Alaa A.-M. Abdel-Aziz ^{a,c}, Magda A. El-Sherbeny ^{c,d}, C. Van Alsenoy ^f

^a Department of Pharmaceutical Chemistry, College of Pharmacy, King Saud University, Riyadh 11451, Saudi Arabia

^b Department of Organic Chemistry, Faculty of Pharmacy, Al-Azhar University, Cairo 11884, Egypt

^c Department of Medicinal Chemistry, Faculty of Pharmacy, University of Mansoura, Mansoura, Egypt

^d Department of Pharmaceutical Chemistry, College of Pharmacy, Delta University for Science and Technology, Gamasa City, Egypt

^e Department of Physics, Fatima Mata National College, Kollam, Kerala, India

^f Department of Chemistry, University of Antwerp, Groenenborgerlaan 171, B-2020 Antwerp, Belgium



ARTICLE INFO

Article history:

Received 22 August 2015

Received in revised form

9 February 2016

Accepted 9 February 2016

Available online 11 February 2016

Keywords:

DFT

FT-IR

FT-Raman

Quinazoline

Molecular docking

ABSTRACT

A comprehensive structural and vibrational study of 2-(4-oxo-3-phenethyl-3,4-dihydroquinazolin-2-ylthio)-N-(3,4,5-trimethoxyphenyl) acetamide is reported. FT-IR and FT-Raman wavenumbers were compared with the theoretical values obtained from DFT calculations. Theoretical values agree well with the experimental values. Molecular electrostatic potential, frontier molecular orbital analysis and nonlinear optical properties were investigated using theoretical calculations. Natural bond orbital analysis shows that charge in electron density in σ^* and π^* antibonding orbitals and E(2) energies confirms the occurrence of intermolecular charge transfer within the molecule. Nonlinear optical property has also been observed by predicting the first and second order hyperpolarizability parameters. As can be seen from the molecular electrostatic potential map of the title molecule, negative region is mainly localized over the carbonyl groups and the mono substituted phenyl ring and the maximum positive region is localized on the NH and hydrogen atoms. Molecular docking results show that the docked ligand title compound forms a stable complex with BRCA2 complex and gives a binding affinity value of -7.6 kcal/mol and results suggest that the compound might exhibit inhibitory activity against BRCA2 complex.

© 2016 Elsevier B.V. All rights reserved.

1. Introduction

Quinazolines are widely used for the extraction and analytical determination of metal ions and nitraquinazone, a quinazoline derivative has been found to possess potent phosphodiesterase inhibitory activity [1] which is potentially useful in the treatment of asthma [2]. Phenyl acetamide derivatives are important and biologically active compounds and have been reported as possible metabolites of antimicrobial active benzoxazoles [3]. These derivatives show various types of biological properties such as

antihelminthic, antihistaminic, antifungal and antibacterial [3]. Quinazoline derivatives have been reported for their anti-bacterial, anti-fungal, anti-HIV [4,5], anthelmintic [6], anti-tubercular [7], hypotensive [8], anti-convulsant [9], anti-fibrillatory [10], diuretic [11] and antiviral [12–14] activities. Among a wide variety of nitrogen heterocycles that have been explored for developing pharmaceutically important molecules, the quinazolines have played an important role in medicinal chemistry and subsequently emerged as a pharmacophore [15]. In the present study, FT-IR and FT-Raman spectra, NBO, MEP and NLO properties of the title compound were reported. Due to the different potential biological activities of the title compound molecular docking of the title compound is also reported.

* Corresponding author.

E-mail address: cyhyp@rediffmail.com (C. Yohannan Panicker).

2. Experimental details

A mixture of 2-mercaptop-3-phenethylquinazolin-4(3*H*)-one (2 mmol, 564 mg) and 2-chloro-N-(3,4,5-trimethoxyphenyl)acetamide (2.1 mmol, 544 mg) in 15 ml acetone containing anhydrous potassium carbonate (3 mmol, 415 mg) was stirred at room temperature for 12 h. The reaction mixture was filtered, the solvent was removed under reduced pressure and the solid obtained was dried and recrystallized from ethanol. Mp: 218–219 °C, yield 94%. ¹H NMR (DMSO-d₆): δ 10.39 (s, 1H), 8.52 (d, 1H, *J* = 3.0 Hz), 8.07 (d, 1H, *J* = 7.5 Hz), 7.80–7.73 (m, 2H), 7.52 (d, 1H, *J* = 8.0 Hz), 7.44 (t, 1H, *J* = 7.5 Hz), 7.34 (d, 1H, *J* = 7.5 Hz), 7.27 (t, 1H, *J* = 5.0, 6.0 Hz), 7.01 (s, 2H), 4.45 (t, 2H, *J* = 7.5, 8.0 Hz), 4.21 (s, 2H), 3.73 (s, 6H), 3.66 (s, 3H), 3.20 (t, 2H, *J* = 7.5, 8.0 Hz). ¹³C NMR (DMSO-d₆): δ: 35.2, 36.9, 43.9, 55.6, 60.0, 79.1, 96.9, 118.7, 121.9, 123.2, 125.7, 126.4, 133.5, 134.6, 135.1, 136.7, 146.6, 149.1, 152.7, 156.0, 157.5, 160.4, 165.5. MS: M⁺ = 505. The FT-IR spectrum (Fig. 1) was recorded using KBr pellets on a DR/Jasco FT-IR 6300 spectrometer. The FT-Raman spectrum (Fig. 2) was obtained on a Bruker RFS 100/s, Germany. For excitation of the spectrum the emission of Nd:YAG laser was used, excitation wavelength was 1064 nm, maximal power was 150 mW and measurement was carried out on solid sample (Fig. 3).

3. Computational details

Calculations of the title compound were carried out using Gaussian 09 software [16] by utilizing Becke's three parameter hybrid model with the Lee-Yang-Parr correlation functional (B3LYP) method. The 6-311++G(d,p) (5D, 7F) basis set was employed to predict the molecular structure and vibrational wave numbers [17,18]. The DFT method tends to overestimate the fundamental modes; therefore scaling factor (0.9613) has to be used for obtaining a considerably better agreement with experimental data [19] and the optimized geometrical parameters are given in Table 1. The assignments of the calculated wave numbers are aided by the animation option of GAUSSVIEW program [20] and the potential energy distribution (PED) is calculated with the help of GAR2PED software package [21].

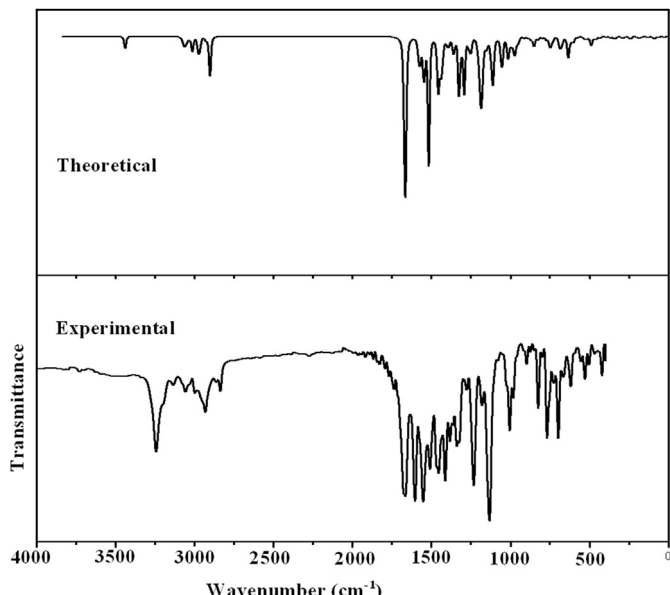


Fig. 1. FT-IR spectrum of 2-(4-oxo-3-phenethyl-3,4-dihydroquinazolin-2-ylthio)-N-(3,4,5-trimethoxyphenyl) acetamide.

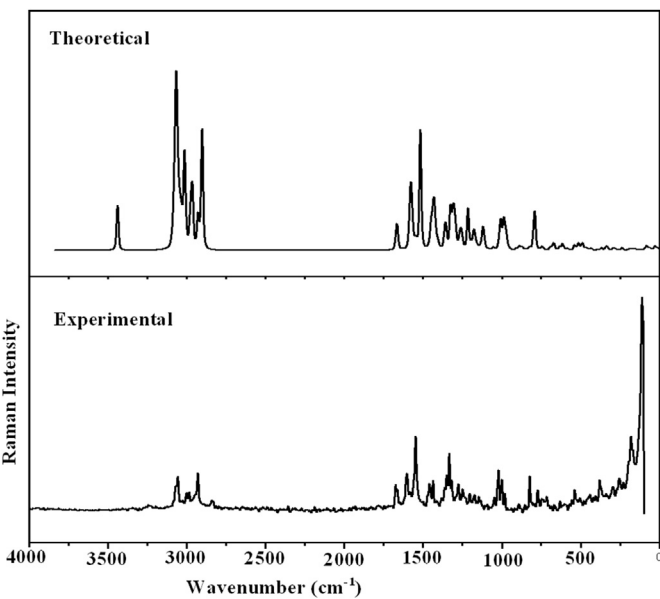


Fig. 2. FT-Raman spectrum of 2-(4-oxo-3-phenethyl-3,4-dihydroquinazolin-2-ylthio)-N-(3,4,5-trimethoxyphenyl) acetamide.

4. Results and discussion

4.1. IR and Raman spectra

The calculated (scaled) wave numbers, observed IR, Raman bands and assignments are given in Table 2. The C=O stretching mode [22–24] is expected in the region 1750–1650 cm⁻¹ and in the present case these modes appears at 1670 cm⁻¹ in the IR spectrum, and at 1675, 1664 cm⁻¹ in the Raman spectrum. The DFT calculations give these modes at 1670 and 1663 cm⁻¹. The in-plane and out-of-plane C=O bending modes are expected in the regions 625 ± 70 and 540 ± 80 cm⁻¹, respectively [22]. For the title compound, the C=O deformation bands are observed at 700, 618 cm⁻¹ in the IR spectrum, 618 cm⁻¹ in the Raman spectrum and at 693, 636, 618, 611 cm⁻¹ theoretically. The C—O—C stretching vibrations are expected in the range 1200–850 cm⁻¹ [22,25]. The skeletal C—O deformation can be found in the region 320 ± 50 cm⁻¹ [22]. As expected, the asymmetric and symmetric C—O—C vibrations are assigned at 1198, 1009, 978, 948, 911, 848 cm⁻¹ theoretically for the title compound, which is in agreement with the literature [24]. Experimentally bands are observed at 915 cm⁻¹ in the IR spectrum and at 1201, 980, 915 cm⁻¹ in the Raman spectrum.

The N—H stretching vibrations give rise to bands at 3500–3300 cm⁻¹ [26]. According to Roeges the N—H stretching vibration appears strongly and broadly in the region 3390 ± 60 cm⁻¹ [22]. For the title compound N—H stretching mode is assigned at 3439 cm⁻¹ theoretically and a strong band is observed in the IR spectrum at 3243 cm⁻¹ and at 3235 cm⁻¹ in the Raman spectrum. Mary et al. [27] reported a band at 3343 cm⁻¹ in the IR spectrum, 3340 cm⁻¹ in Raman spectrum and 3433 cm⁻¹ theoretically as N—H stretching mode. For the title compound the band at 1409 cm⁻¹ (DFT) is assigned as N—H in-plane bending mode and experimentally at 1411 cm⁻¹ in both the spectra. The out-of-plane bending of NH is expected around 650 ± 50 cm⁻¹ [22]. In the present case the band at 665 (IR), 667 (Raman) and 669 cm⁻¹ (DFT) is assigned as out-of-plane bending of N—H.

Louran et al. [28] reported a value at 1220 cm⁻¹ for ν C—N for poly aniline. In the case of aromatic amines a strong C—N stretching absorption is observed in the region in 1342–1266 cm⁻¹ [23,24].

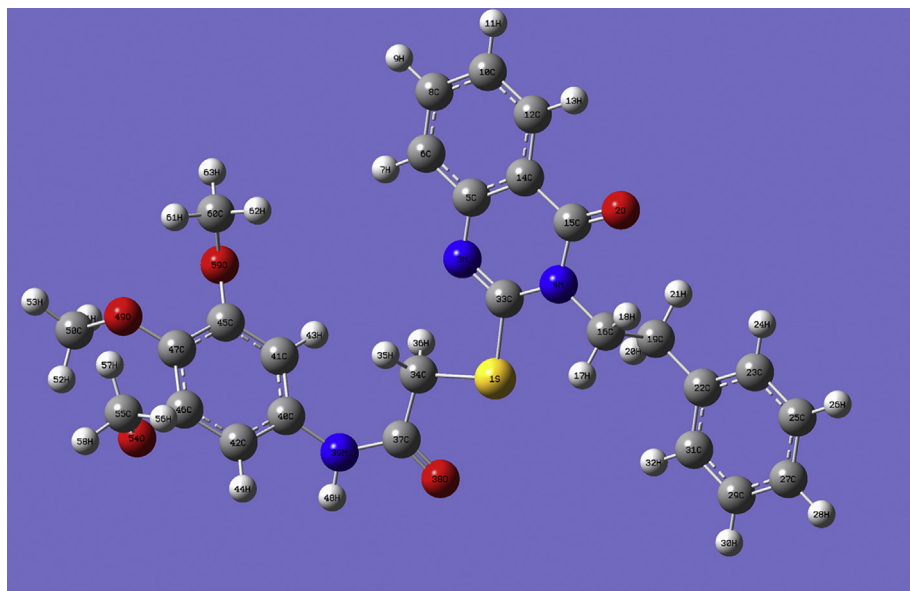


Fig. 3. Optimized geometry of 2-(4-oxo-3-phenethyl-3,4-dihydroquinazolin-2-ylthio)-N-(3,4,5-trimethoxyphenyl) acetamide.

Table 1

Optimized geometrical parameters of 2-(4-oxo-3-phenethyl-3,4-dihydroquinazolin-2-ylthio)-N-(3,4,5-trimethoxyphenyl) acetamide.

Bond lengths (Å)					
S1–C33	1.7853	S1–C34	1.8304	O2–C15	1.2205
N3–C5	1.3825	N3–C33	1.2924	N4–C15	1.4157
N4–C16	1.4765	N4–C33	1.3859	C5–C6	1.4082
C5–C14	1.4088	C6–H7	1.0833	C6–C8	1.3832
C8–H9	1.0846	C8–C10	1.4056	C10–H11	1.0836
C10–C12	1.3833	C12–H13	1.0831	C12–C14	1.4034
C14–C15	1.4628	C16–H17	1.0902	C16–H18	1.0887
C16–C19	1.5408	C19–H20	1.0932	C19–H21	1.0926
C19–C22	1.5124	C22–C23	1.3996	C22–C31	1.3995
C23–H24	1.0856	C23–C25	1.3936	C25–H26	1.0845
C25–C27	1.3941	C27–H28	1.0842	C27–C29	1.3939
C29–H30	1.0844	C29–C31	1.3938	C31–H32	1.0856
C34–H35	1.0879	C34–H36	1.0906	C34–C37	1.5216
C37–O38	1.2192	C37–N39	1.3759	N39–C40	1.4215
N39–H48	1.0125	C40–C41	1.3947	C40–C42	1.3973
C41–H43	1.0816	C41–C45	1.3951	C42–H44	1.0834
C42–C46	1.3919	C45–C47	1.4031	C45–O59	1.3701
C46–C47	1.4045	C46–O54	1.3715	C47–O49	1.374
O49–C50	1.4391	C50–H51	1.0937	C50–H52	1.0932
C50–H53	1.0895	O54–C55	1.4372	C55–H56	1.0949
C55–H57	1.0917	C55–H58	1.0892	O59–C60	1.4367
C60–H61	1.0912	C60–H62	1.0951	C60–H63	1.0893
Bond lengths (Å)					
S1–C33	1.7853	S1–C34	1.8304	O2–C15	1.2205
N3–C5	1.3825	N3–C33	1.2924	N4–C15	1.4157
N4–C16	1.4765	N4–C33	1.3859	C5–C6	1.4082
C5–C14	1.4088	C6–H7	1.0833	C6–C8	1.3832
C8–H9	1.0846	C8–C10	1.4056	C10–H11	1.0836
C10–C12	1.3833	C12–H13	1.0831	C12–C14	1.4034
C14–C15	1.4628	C16–H17	1.0902	C16–H18	1.0887
C16–C19	1.5408	C19–H20	1.0932	C19–H21	1.0926
C19–C22	1.5124	C22–C23	1.3996	C22–C31	1.3995
C23–H24	1.0856	C23–C25	1.3936	C25–H26	1.0845
C25–C27	1.3941	C27–H28	1.0842	C27–C29	1.3939
C29–H30	1.0844	C29–C31	1.3938	C31–H32	1.0856
C34–H35	1.0879	C34–H36	1.0906	C34–C37	1.5216
C37–O38	1.2192	C37–N39	1.3759	N39–C40	1.4215
N39–H48	1.0125	C40–C41	1.3947	C40–C42	1.3973
C41–H43	1.0816	C41–C45	1.3951	C42–H44	1.0834
C42–C46	1.3919	C45–C47	1.4031	C45–O59	1.3701
C46–C47	1.4045	C46–O54	1.3715	C47–O49	1.374
O49–C50	1.4391	C50–H51	1.0937	C50–H52	1.0932
C50–H53	1.0895	O54–C55	1.4372	C55–H56	1.0949
C55–H57	1.0917	C55–H58	1.0892	O59–C60	1.4367

(continued on next page)

Table 1 (continued)

C60–H61	1.0912	C60–H62	1.0951	C60–H63	1.0893
Torsion angles (°)					
C34–S1–C33–N3	−2.7	C34–S1–C33–N4	178.0	C33–S1–C34–H35	−57.4
C33–S1–C34–H36	60.1	C33–S1–C34–C37	179.7	C33–N3–C5–C6	179.8
C33–N3–C5–C14	0.1	C5–N3–C33–S1	−179.1	C5–N3–C33–N4	0.2
C16–N4–C15–O2	−0.4	C16–N4–C15–C14	179.6	C33–N4–C15–O2	−178.7
C33–N4–C15–C14	1.3	C15–N4–C16–H17	149.3	C15–N4–C16–H18	33.2
C15–N4–C16–C19	−87.3	C33–N4–C16–H17	−32.4	C33–N4–C16–H18	−148.5
C33–N4–C16–C19	91.1	C15–N4–C33–S1	178.4	C15–N4–C33–N3	−0.9
C16–N4–C33–S1	0.1	C16–N4–C33–N3	−179.2	N3–C5–C6–H7	−0.3
N3–C5–C6–C8	180.0	C14–C5–C6–H7	179.5	C14–C5–C6–C8	−0.2
N3–C5–C14–C12	180.0	N3–C5–C14–C15	0.4	C6–C5–C14–C12	0.2
C6–C5–C14–C15	−179.4	C5–C6–C8–H9	179.9	C5–C6–C8–C10	0.0
H7–C6–C8–H9	0.2	H7–C6–C8–C10	−179.7	C6–C8–C10–H11	180.0
C6–C8–C10–C12	0.2	H9–C8–C10–H11	0.1	H9–C8–C10–C12	−179.7
C8–C10–C12–H13	179.7	C8–C10–C12–C14	−0.2	H11–C10–C12–H13	−0.1
H11–C10–C12–C14	180.0	C10–C12–C14–C5	0.0	C10–C12–C14–C15	179.6
H13–C12–C14–C5	−179.9	H13–C12–C14–C15	−0.4	C5–C14–C15–O2	178.9
C5–C14–C15–N4	−1.0	C12–C14–C15–O2	−0.6	C12–C14–C15–N4	179.4
N4–C16–C19–H20	−58.0	N4–C16–C19–H21	59.2	N4–C16–C19–C22	−179.6
H17–C16–C19–H20	64.1	H17–C16–C19–H21	−178.7	H17–C16–C19–C22	−57.5
H18–C16–C19–H20	−176.5	H18–C16–C19–H21	−59.4	H18–C16–C19–C22	61.9
C16–C19–C22–C23	−88.0	C16–C19–C22–C31	90.3	H20–C19–C22–C23	150.8
H20–C19–C22–C31	−30.9	H21–C19–C22–C23	32.2	H21–C19–C22–C31	−149.5
C19–C22–C23–H24	−1.9	C19–C22–C23–C25	178.4	C31–C22–C23–H24	179.7
C31–C22–C23–C25	0.1	C19–C22–C31–C29	−178.4	C19–C22–C31–H32	2.0
C23–C22–C31–C29	−0.1	C23–C22–C31–H32	−179.6	C22–C23–C25–H26	179.7
C22–C23–C25–C27	−0.1	H24–C23–C25–H26	0.0	H24–C23–C25–C27	−179.8
C23–C25–C27–H28	179.8	C23–C25–C27–C29	0.1	H26–C25–C27–H28	0.0
H26–C25–C27–C29	−179.7	C25–C27–C29–H30	179.7	C25–C27–C29–C31	−0.1
H28–C27–C29–H30	−0.0	H28–C27–C29–C31	−179.8	C27–C29–C31–C22	0.0
C27–C29–C31–H32	179.6	H30–C29–C31–C22	−179.7	H30–C29–C31–H32	−0.1
S1–C34–C37–O38	−23.4	S1–C34–C37–N39	156.5	H35–C34–C37–O38	−144.6
H35–C34–C37–N39	35.3	H36–C34–C37–O38	95.0	H36–C34–C37–N39	−85.1
C34–C37–N39–C40	−3.9	C34–C37–N39–H48	−174.6	O38–C37–N39–C40	176.0
O38–C37–N39–H48	5.3	C37–N39–C40–C41	51.9	C37–N39–C40–C42	−130.2
H48–N39–C40–C41	−137.8	H48–N39–C40–C42	40.2	N39–C40–C41–H43	0.8
N39–C40–C41–C45	178.4	C42–C40–C41–H43	−177.1	C42–C40–C41–C45	0.5
N39–C40–C42–H44	2.9	N39–C40–C42–C46	−177.3	C41–C40–C42–H44	−179.2
C41–C40–C42–C46	0.6	C40–C41–C45–C47	−1.9	C40–C41–C45–O59	−176.6
H43–C41–C45–C47	175.7	H43–C41–C45–O59	1.0	C40–C42–C46–C47	−0.3
C40–C42–C46–O54	176.5	H44–C42–C46–C47	179.5	H44–C42–C46–O54	−3.7
C41–C45–C47–C46	2.2	C41–C45–C47–O49	−178.0	O59–C45–C47–C46	176.8
O59–C45–C47–O49	−3.5	C41–C45–O59–C60	−117.2	C47–C45–O59–C60	68.1
C42–C46–C47–C45	−1.1	C42–C46–C47–O49	179.2	O54–C46–C47–C45	−177.9
O54–C46–C47–O49	2.4	C42–C46–O54–C55	113.0	C47–C46–O54–C55	−70.2
C45–C47–O49–C50	96.6	C46–C47–O49–C50	−83.6	C47–O49–C50–H51	−61.7
C47–O49–C50–H52	60.5	C47–O49–C50–H53	179.5	C46–O54–C55–H56	−62.1
C46–O54–C55–H57	60.2	C46–O54–C55–H58	179.6	C45–O59–C60–H61	−61.7
C45–O59–C60–H62	60.5	C45–O59–C60–H63	178.8		

Varghese et al. [29] reported νC–N mode at 1203 cm^{−1} in the IR spectrum and at 1208 cm^{−1} theoretically. For the title compound, the C–N stretching modes are assigned at 1335, 1323, 1272, 953 cm^{−1} in IR, 1333, 1319, 1272, 1158, 1107 cm^{−1} in Raman and in the range 1326–952 cm^{−1} theoretically which are in agreement with literature [22–24]. The C=N stretching mode is observed at 1515 cm^{−1} in IR, 1520 cm^{−1} in Raman and 1517 cm^{−1} theoretically as expected [22]. For the title compound C–S stretching modes are observed at 770 cm^{−1} in the IR spectrum, and at 770, 636 cm^{−1} theoretically as expected [22].

The stretching vibrations of the CH₂ group (the asymmetric and symmetric stretch) and deformation modes of CH₂ group (scissoring, wagging, twisting and rocking modes) appears in the regions 3000 ± 20, 2900 ± 25, 1450 ± 30, 1330 ± 35, 1245 ± 45, 780 ± 55 cm^{−1} respectively [22–24]. The CH₂ stretching modes are observed at 3036, 3008, 2955 cm^{−1} in the Raman spectrum, 3034, 3005 cm^{−1} in the IR spectrum and in the range 3035–2902 cm^{−1} theoretically. The deformation modes of CH₂ are assigned at 1388, 1323, 1242 cm^{−1} in the IR spectrum, 1388, 1351, 1319, 853, 743 cm^{−1} in the Raman spectrum and in the ranges 1445–1391 (scissoring),

1354–1306 (wagging), 1292–1152 (twisting), 976–740 (rocking) cm^{−1} theoretically as expected [22–24].

For the title compound, the CH₃ stretching modes are assigned at 3034, 3022, 2984, 2931 cm^{−1} in the IR spectrum, 3023, 2982, 2929 cm^{−1} in the Raman spectrum and in the range 3033–2903 cm^{−1} theoretically and these modes are expected in the region 2900–3050 cm^{−1} according to literature [22]. The deformation modes of the methyl group of the title compound are assigned as 1411 cm^{−1} in the IR spectrum and 1440, 1411, 1148, 1121 cm^{−1} in the Raman spectrum and in the ranges 1452–1400 (scissoring) and 1170–1110 cm^{−1} (rocking) theoretically as expected [22].

In the following discussion, the poly, ortho, mono-substituted phenyl rings are designated as PhI, PhII and PhIII respectively and the quinazoline ring as PhIV. For phenyl rings, the C–H stretching modes are expected above 3000 cm^{−1} [22] and for the title compound, the CH stretching modes are assigned in the range 3077–3070 for PhI, 3087–3045 for PhII and 3065–3014 cm^{−1} for PhIII rings theoretically. Experimentally bands are observed at 3056 cm^{−1} in IR and 3070, 3058 cm^{−1} in Raman spectrum. The

Table 2

Calculated (scaled) wavenumbers, observed IR, Raman bands and assignments of 2-(4-oxo-3-phenethyl-3,4-dihydroquinazolin-2-ylthio)-N-(3,4,5-trimethoxyphenyl) acetamide.

B3LYP/6-311++G(d,p) (5D,7F)				IR $\nu(\text{cm}^{-1})$	Raman $\nu(\text{cm}^{-1})$	Assignments ^a
$\nu(\text{cm}^{-1})$	b $\nu(\text{cm}^{-1})_c$	IR _I	R _A	$\nu(\text{cm}^{-1})$	$\nu(\text{cm}^{-1})$	—
3577	3439	44.66	173.54	3243	3235	$\nu\text{NH}(100)$
3211	3087	1.17	66.17	—	—	$\nu\text{CHII}(95)$
3201	3077	9.82	244.22	—	—	$\nu\text{CHI}(99)$
3193	3070	9.14	120.43	—	3070	$\nu\text{CHI}(99)$
3191	3067	0.78	72.78	—	—	$\nu\text{CHII}(99)$
3188	3065	19.96	363.03	—	—	$\nu\text{CHIII}(92)$
3183	3060	9.47	149.48	—	3058	$\nu\text{CHII}(100)$
3177	3054	25.02	48.66	3056	—	$\nu\text{CHIII}(99)$
3168	3045	6.88	93.68	—	—	$\nu\text{CHII}(98)$
3167	3045	4.09	73.39	—	—	$\nu\text{CHIII}(94)$
3157	3035	0.81	93.52	3034	3036	$\nu\text{CH}_2(100)$
3155	3033	6.79	16.86	3034	—	$\nu\text{CH}_3(100)$
3141	3020	0.32	45.34	3022	3023	$\nu\text{CH}_3(100)$
3136	3015	5.60	12.53	—	—	$\nu\text{CHIII}(91)$
3136	3015	8.86	118.53	—	—	$\nu\text{CH}_3(99)$
3135	3014	26.55	95.39	—	—	$\nu\text{CHIII}(99)$
3132	3010	22.88	132.89	3005	3008	$\nu\text{CH}_2(91)$
3097	2977	32.36	57.49	2984	2982	$\nu\text{CH}_3(96)$
3095	2975	21.27	45.32	—	—	$\nu\text{CH}_3(98)$
3092	2972	19.61	34.24	—	—	$\nu\text{CH}_3(96)$
3091	2972	9.24	37.79	—	—	$\nu\text{CH}_2(99)$
3083	2964	12.09	38.57	—	—	$\nu\text{CH}_2(98)$
3083	2963	10.68	131.15	—	2955	$\nu\text{CH}_2(95)$
3047	2929	11.09	108.32	2931	2929	$\nu\text{CH}_3(100)$
3022	2905	50.84	195.26	—	—	$\nu\text{CH}_3(95)$
3020	2903	75.67	197.04	—	—	$\nu\text{CH}_3(95)$
3019	2902	41.52	71.27	—	—	$\nu\text{CH}_2(99)$
1737	1670	473.91	45.95	1670	1675	$\nu\text{C} = \text{O}(64), \nu\text{NH}(17)$
1730	1663	414.33	45.44	—	1664	$\nu\text{C} = \text{O}(52)$
1646	1583	48.93	71.69	—	1582	$\nu\text{PhII}(56), \delta\text{CHII}(14)$
1644	1580	8.11	66.61	—	—	$\nu\text{PhII}(61), \delta\text{CHIII}(18)$
1637	1573	127.47	131.29	—	—	$\nu\text{PhII}(42), \delta\text{PhII}(10)$
1623	1560	1.05	10.35	—	—	$\nu\text{PhII}(67), \delta\text{CHIII}(20)$
1612	1549	118.62	9.63	1552	—	$\nu\text{PhII}(56), \delta\text{PhII}(12)$
1608	1546	105.75	16.88	—	1547	$\nu\text{PhII}(50), \nu\text{C} = \text{O}(15)$
1579	1517	484.97	279.5	1515	1520	$\nu\text{C} = \text{N}(46), \nu\text{PhIII}(22)$
1526	1467	17.80	2.02	1468	1470	$\delta\text{CHIII}(14), \nu\text{PhIII}(64)$
1517	1458	181.35	3.67	1456	1460	$\delta\text{CH}_3(30), \nu\text{PhII}(59)$
1511	1452	8.48	17.20	—	—	$\delta\text{CH}_3(91)$
1509	1451	10.47	17.25	—	—	$\delta\text{CH}_3(55)$
1503	1445	14.63	23.99	—	—	$\delta\text{CH}_2(88)$
1503	1444	21.84	7.15	—	—	$\delta\text{CH}_2(87)$
1501	1443	79.78	29.21	—	—	$\delta\text{CH}_2(84)$
1500	1442	47.59	15.54	—	1440	$\delta\text{CH}_3(92)$
1490	1432	8.36	14.32	—	—	$\delta\text{CHII}(17), \nu\text{PhII}(55)$
1488	1431	7.74	14.25	—	—	$\delta\text{CH}_3(86)$
1488	1430	20.24	9.43	—	—	$\delta\text{CH}_3(89)$
1487	1430	21.00	5.85	—	—	$\delta\text{CHII}(15), \nu\text{PhII}(57)$
1486	1428	26.86	77.03	—	—	$\delta\text{CHIII}(22), \nu\text{PhIII}(62)$
1483	1426	0.72	5.86	—	—	$\delta\text{CH}_3(63), \nu\text{NH}(12)$
1478	1421	2.72	16.32	—	—	$\delta\text{CH}_3(72)$
1466	1409	5.15	24.92	1411	1411	$\delta\text{CH}_3(44), \nu\text{NH}(40)$
1457	1400	31.53	3.72	—	—	$\delta\text{CH}_3(58), \nu\text{NH}(12), \delta\text{CH}_2(10)$
1447	1391	32.53	0.97	1388	1388	$\delta\text{CH}_2(75)$
1418	1363	52.30	40.84	1365	1363	$\nu\text{PhII}(58), \delta\text{CH}_3(24), \delta\text{CHII}(10)$
1409	1354	21.99	37.14	—	1351	$\delta\text{CH}_2(78)$
1380	1326	173.26	72.71	1335	1333	$\nu\text{CN}(41), \delta\text{CH}_2(20), \nu\text{CC}(13)$
1377	1323	101.50	40.28	1323	1319	$\delta\text{CH}_2(44), \nu\text{CN}(41)$
1363	1310	5.50	11.07	—	—	$\delta\text{CHIII}(47), \delta\text{CH}_2(13)$
1358	1306	37.36	135.84	—	—	$\delta\text{CH}_2(52), \nu\text{CO}(24)$
1344	1292	207.97	28.86	—	—	$\delta\text{CH}_2(81)$
1342	1290	0.82	2.14	—	1292	$\delta\text{CHII}(54), \nu\text{CC}(13)$
1321	1270	5.98	20.31	1272	1272	$\nu\text{CN}(44), \delta\text{CH}_2(20), \delta\text{CHII}(10)$
1316	1265	27.22	17.87	—	—	$\delta\text{CH}_2(43), \nu\text{CN}(10), \nu\text{PhII}(20)$
1306	1255	34.14	47.81	—	1253	$\nu\text{PhII}(40), \delta\text{CHII}(12)$
1299	1248	39.96	1.58	1242	—	$\delta\text{CH}_2(41), \nu\text{CN}(19)$
1265	1216	4.33	88.60	—	—	$\nu\text{PhII}(50), \delta\text{CHIII}(10)$
1255	1206	24.61	2.49	—	—	$\delta\text{CHI}(54), \nu\text{CO}(14), \nu\text{PhII}(12)$
1246	1198	58.03	8.79	—	1201	$\nu\text{CO}(46), \delta\text{CHI}(25)$
1235	1188	216.99	4.11	—	—	$\nu\text{CN}(46), \nu\text{PhII}(11), \delta\text{CHII}(11)$
1226	1179	146.43	13.90	1181	—	$\nu\text{CC}(37), \delta\text{CHIII}(51)$

(continued on next page)

Table 2 (continued)

B3LYP/6-311++G(d,p) (5D,7F)				IR $\nu(\text{cm}^{-1})$	Raman $\nu(\text{cm}^{-1})$	Assignments ^a
$\nu(\text{cm}^{-1})$	b $\nu(\text{cm}^{-1})_c$	IR _I	R _A	$\nu(\text{cm}^{-1})$	$\nu(\text{cm}^{-1})$	—
1224	1176	1.26	47.08	—	1174	$\delta\text{CH}_3(56), \nu\text{PhIII}(21)$
1217	1170	21.40	2.46	—	—	$\delta\text{CH}_3(74)$
1209	1162	4.08	5.20	—	—	$\delta\text{CH}_3(65)$
1204	1157	0.10	3.71	—	1158	$\delta\text{CH}_2(46), \nu\text{CN}(42)$
1199	1152	26.22	2.04	—	—	$\delta\text{CH}_2(42), \nu\text{PhI}(50)$
1196	1150	29.20	2.51	—	1148	$\delta\text{CH}_3(68)$
1182	1136	0.65	4.50	—	1135	$\delta\text{CH}_2(23), \nu\text{PhI}(72)$
1169	1124	51.90	7.34	1127	—	$\delta\text{CH}_3(44), \nu\text{PhIII}(18)$
1168	1123	6.26	6.22	—	—	$\delta\text{CH}_3(62), \nu\text{PhII}(14)$
1167	1122	10.53	9.14	—	1121	$\nu\text{CN}(12), \delta\text{CH}_3(19), \delta\text{CHI}(48)$
1167	1122	29.40	27.29	—	1121	$\delta\text{CH}_3(96)$
1165	1120	2.39	5.83	—	—	$\delta\text{CH}_3(86)$
1155	1110	4.55	4.32	—	—	$\delta\text{CH}_3(95)$
1154	1109	180.92	11.73	—	1107	$\nu\text{CN}(42), \delta\text{CH}_2(11)$
1127	1084	3.28	2.36	1080	1080	$\nu\text{PhII}(54), \delta\text{CHII}(21)$
1105	1062	12.14	0.84	—	—	$\nu\text{PhIII}(38), \delta\text{CHIII}(24), \delta\text{CH}_2(11)$
1097	1055	173.78	7.27	—	1050	$\delta\text{CHII}(83), \tau\text{PhII}(14)$
1059	1018	82.45	19.22	1020	1021	$\delta\text{CHIII}(78), \tau\text{PhIII}(20)$
1050	1009	7.28	18.51	—	—	$\nu\text{CO}(66)$
1047	1007	8.27	37.47	1005	1002	$\gamma\text{CHII}(87)$
1035	995	37.46	1.46	—	—	$\gamma\text{CHIII}(91)$
1030	990	3.93	48.32	988	—	$\delta\text{PhIII}(17), \nu\text{PhIII}(55)$
1017	978	0.04	48.89	—	980	$\nu\text{CO}(44), \nu\text{PhI}(42)$
1015	976	97.62	14.44	—	—	$\delta\text{CH}_2(46), \nu\text{PhIII}(14)$
1004	965	10.74	2.83	—	967	$\nu\text{PhII}(14), \nu\text{CC}(36)$
1004	965	0.44	0.20	—	—	$\nu\text{PhII}(22), \gamma\text{CHII}(61)$
1000	962	0.69	1.73	—	—	$\gamma\text{CHIII}(60), \nu\text{PhIII}(16)$
990	952	33.15	2.81	953	—	$\nu\text{CN}(48), \nu\text{PhII}(22), \delta\text{PhIV}(14)$
986	948	0.05	0.01	—	—	$\nu\text{CO}(76), \delta\text{PhI}(10)$
985	947	0.82	0.11	—	942	$\gamma\text{CHIII}(70), \nu\text{CC}(13)$
947	911	6.09	3.73	915	915	$\nu\text{CO}(50), \gamma\text{CHI}(13)$
929	893	1.22	4.80	895	892	$\gamma\text{CHI}(80), \tau\text{PhI}(10)$
920	885	7.27	6.88	—	—	$\gamma\text{CHI}(58), \tau\text{PhI}(17)$
905	870	11.98	5.56	872	874	$\gamma\text{CHII}(73), \tau\text{PhII}(10)$
887	853	1.49	0.11	—	853	$\delta\text{CH}_2(70), \gamma\text{C = O}(23)$
886	852	26.66	1.39	850	853	$\gamma\text{CHIII}(92)$
882	848	12.90	0.27	—	—	$\nu\text{CO}(72), \delta\text{PhI}(10)$
869	835	1.98	1.88	—	836	$\delta\text{PhII}(26), \delta\text{PhIV}(11), \nu\text{CN}(13)$
859	826	5.70	2.48	826	—	$\nu\text{CC}(44), \nu\text{CN}(10)$
858	825	5.31	2.15	826	823	$\tau\text{PhIV}(10), \gamma\text{C = O}(10), \delta\text{PhII}(10)$
832	800	5.30	23.00	798	—	$\tau\text{PhIV}(25), \gamma\text{C = O}(22), \tau\text{PhII}(17)$
823	791	2.10	67.05	—	792	$\nu\text{CC}(10), \nu\text{CS}(10), \delta_c = \text{O}(10)$
804	773	11.96	0.63	—	773	$\gamma\text{CHII}(81)$
801	770	0.87	0.73	770	—	$\nu\text{CS}(45), \tau\text{PhI}(19), \delta\text{CN}(15)$
781	751	56.26	0.96	—	—	$\tau\text{PhI}(38), \gamma\text{CO}(40)$
779	749	0.20	4.77	—	—	$\tau\text{PhII}(20), \gamma\text{CHIII}(55)$
770	740	7.63	3.00	—	743	$\delta\text{CH}_2(63)$
763	734	18.77	1.31	731	729	$\nu\text{CS}(12), \tau\text{PhI}(10), \delta\text{CH}_2(10)$
721	693	16.66	7.05	700	—	$\tau\text{PhII}(37), \gamma\text{C = O}(36)$
712	685	41.62	1.91	—	685	$\tau\text{PhIII}(55), \gamma\text{CHIII}(28)$
705	678	17.38	5.05	—	—	$\delta\text{PhII}(21), \tau\text{PhIII}(16), \delta\text{CN}(10)$
696	669	10.31	11.67	665	667	$\gamma\text{NH}(47), \gamma\text{C = O}(10), \gamma\text{CO}(14)$
673	647	9.38	0.52	—	—	$\gamma\text{CN}(26), \tau\text{PhI}(20)$
661	636	3.14	1.38	—	—	$\nu\text{CS}(41), \gamma\text{C = O}(33)$
659	633	89.92	5.31	—	631	$\tau\text{PhI}(18), \gamma\text{CO}(36), \gamma\text{NH}(10), \delta\text{CO}(12)$
643	618	7.61	8.88	618	618	$\delta\text{PhII}(24), \delta_c = \text{O}(35), \delta\text{CN}(10), \delta\text{CS}(10)$
638	614	4.39	0.72	—	—	$\delta\text{PhIII}(81)$
636	611	0.11	4.07	—	—	$\tau\text{PhI}(24), \delta_c = \text{O}(34), \gamma\text{CN}(11)$
628	604	28.77	2.09	599	598	$\delta\text{CO}(45), \delta\text{CN}(12), \tau\text{PhI}(11), \gamma\text{CO}(18)$
609	585	1.61	3.09	586	—	$\delta\text{PhII}(45), \delta\text{PhIV}(18)$
601	578	4.30	1.48	—	576	$\delta\text{PhIII}(30), \delta\text{PhII}(10), \delta\text{CS}(10)$
561	540	0.84	8.51	—	538	$\tau\text{PhII}(62), \tau\text{PhIV}(10)$
549	528	14.64	4.71	529	525	$\gamma\text{CO}(18), \delta\text{CO}(28), \delta\text{PhI}(15)$
538	517	7.97	0.61	—	—	$\delta\text{PhIV}(44), \delta\text{PhII}(10)$
533	512	0.74	15.35	510	509	$\tau\text{PhIII}(37), \gamma\text{CC}(25)$
513	493	11.79	2.31	—	—	$\delta_c = \text{O}(17), \tau\text{PhI}(21), \delta\text{CS}(15)$
510	490	31.79	13.54	—	492	$\gamma\text{C = O}(36), \delta\text{PhI}(16), \delta\text{CH}_2(14)$
486	467	16.53	6.67	466	464	$\delta\text{PhI}(28), \gamma\text{C = O}(19), \tau\text{NH}(10)$
473	455	4.61	1.69	—	—	$\tau\text{PhII}(25), \delta\text{PhIV}(25), \delta\text{PhIII}(10)$
453	436	4.53	2.12	—	438	$\tau\text{PhII}(49), \tau\text{PhIV}(21)$
446	428	2.00	1.77	425	423	$\delta\text{CO}(12), \delta\text{CN}(11), \gamma\text{CO}(18)$
414	398	0.28	0.23	—	401	$\tau\text{PhIII}(85)$
407	391	3.31	1.49	—	—	$\delta\text{CN}(49), \delta_c = \text{O}(21)$

Table 2 (continued)

B3LYP/6-311++G(d,p) (5D,7F)				IR	Raman	Assignments ^a
$\nu(\text{cm}^{-1})$	$b \nu(\text{cm}^{-1})_c$	IR _I	R _A	$\nu(\text{cm}^{-1})$	$\nu(\text{cm}^{-1})$	—
385	370	2.04	4.65	—	372	$\delta\text{CS}(32), \delta\text{PhIV}(17), \delta_c = \text{O}(10)$
379	364	6.42	1.31	—	—	$\delta\text{PhI}(31), \gamma\text{CO}(10), \delta\text{CS}(10)$
355	342	8.54	3.58	—	340	$\gamma\text{CN}(24), \tau\text{PhIII}(14), \delta\text{CH}_2(20), \tau\text{PhII}(11)$
348	334	2.10	5.19	—	—	$\tau\text{PhI}(30), \delta\text{CO}(41), \delta\text{CN}(10)$
342	328	0.51	0.46	—	—	$\delta\text{CC}(54), \tau\text{PhI}(22)$
340	327	2.18	1.53	—	325	$\delta\text{CO}(24), \delta\text{CC}(10)$
309	297	1.77	2.94	—	295	$\delta\text{CN}(28), \tau\text{PhI}(16), \tau\text{NH}(10), \delta\text{CO}(17)$
304	292	5.69	0.81	—	—	$\delta\text{CS}(15), \tau\text{PhI}(13), \delta_c = \text{O}(10)$
296	285	1.94	2.34	—	—	$\tau\text{PhII}(42), \tau\text{PhIV}(26)$
291	280	0.33	0.98	—	—	$\tau\text{PhI}(26), \delta\text{CO}(43), \delta\text{PhI}(10)$
281	270	2.70	0.94	—	272	$\delta\text{CS}(10), \tau\text{PhI}(10), \delta\text{PhII}(10), \delta\text{CN}(10)$
252	243	9.74	1.82	—	250	$\tau\text{PhIII}(28), \delta\text{CH}_2(10)$
246	236	4.91	4.10	—	232	$\tau\text{PhI}(16), \tau\text{PhIII}(10), \delta\text{CO}(30)$
206	198	4.58	2.10	—	195	$\gamma\text{CO}(17), \delta\text{CO}(17), \delta\text{CS}(14)$
194	186	4.50	1.43	—	184	$\delta\text{CO}(32), \tau\text{PhI}(15), \gamma\text{CO}(25)$
180	173	5.61	3.45	—	—	$\delta\text{CH}_2(39), \delta\text{CS}(20)$
164	158	0.01	0.63	—	162	$\tau\text{PhIV}(52), \tau\text{PhII}(21)$
161	154	0.54	0.85	—	—	$\tau\text{CH}_2(81)$
159	152	0.18	1.00	—	—	$\gamma\text{CN}(19), \tau\text{PhIV}(29), \delta\text{CH}_2(10)$
154	148	0.36	1.04	—	—	$\tau\text{CH}_3(86)$
138	133	3.46	0.87	—	—	$\tau\text{CH}_3(81)$
127	123	1.84	1.04	—	—	$\gamma\text{CO}(38), \tau\text{CH}_3(23)$
101	97	1.61	0.89	—	107	$\tau\text{PhIV}(48), \tau\text{PhII}(13)$
98	94	5.78	2.38	—	—	$\tau\text{CO}(36), \gamma\text{CC}(10), \delta\text{CH}_2(10)$
90	87	5.53	1.20	—	—	$\gamma\text{CC}(12), \delta\text{CH}_2(13), \tau\text{CO}(21)$
85	82	0.03	4.30	—	—	$\tau\text{CO}(39), \tau\text{NH}(28)$
82	79	1.35	0.55	—	—	$\tau\text{CH}_2(20), \tau\text{CO}(17), \tau\text{PhI}(10)$
81	78	0.31	2.11	—	—	$\tau\text{CO}(17), \tau\text{CH}_2(16), \tau\text{CS}(13), \tau_c = \text{O}(13)$
69	66	1.45	2.91	—	—	$\tau\text{C} = \text{O}(24), \tau\text{NH}(25), \tau\text{CS}(20)$
62	59	1.15	2.99	—	—	$\tau\text{CH}_2(20), \tau\text{CO}(21), \tau\text{PhI}(10), \tau\text{C} = \text{O}(10)$
56	54	1.02	0.58	—	—	$\tau\text{CO}(23), \delta\text{CS}(23), \tau\text{PhI}(12)$
36	35	0.31	0.63	—	—	$\tau\text{CO}(79)$
32	31	1.13	1.93	—	—	$\tau\text{PhIV}(24), \delta\text{CH}_2(21), \tau\text{CC}(12), \gamma\text{CN}(10)$
30	29	0.19	2.95	—	—	$\tau\text{CH}_2(32), \tau\text{CC}(14), \tau\text{CN}(10)$
29	28	1.51	1.98	—	—	$\tau\text{CC}(38), \tau\text{CH}_2(24), \tau\text{CN}(10)$
22	21	1.15	0.85	—	—	$\tau\text{CH}_2(27), \delta\text{CN}(20), \gamma\text{CN}(13)$
16	15	0.40	0.88	—	—	$\tau\text{CH}_2(53), \tau\text{CC}(11)$
9	9	0.09	3.89	—	—	$\tau\text{CN}(51), \tau\text{PhI}(10), \tau\text{CH}_2(10)$
9	9	0.18	0.96	—	—	$\tau\text{C} = \text{O}(40), \tau\text{CN}(31), \tau\text{CS}(10)$

^a ν -strectching; δ -in-plane deformation; γ -out-of-plane deformation; τ -torsion; PhI-poly substituted phenyl ring; PhII-ortho substituted phenyl ring; PhIII- mono-substituted phenyl ring; PhIV-Quinazoline ring; potential energy distribution (%) is given in brackets in the assignment column; The first column with subscript b represents unscaled wavenumbers and second column with subscript c represents scaled wavenumbers.

phenyl ring stretching modes are assigned at 1552, 1456, 1365 (IR), 1460, 1363, 1135 (Raman), in the range 1573–1136 (DFT) for PhI, 1582, 1547, 1253 (Raman), in the range 1583–1255 (DFT) for PhII and 1468 (IR), 1470 (Raman), in the range 1580–1216 cm^{-1} (DFT) for PhIII. The sixth phenyl ring stretching mode, the ring breathing vibration appears as a weak band near 1000 cm^{-1} in mono-, 1,3-di- and 1,3,5-tri substituted benzenes [22,30]. In the otherwise substituted benzenes however, this vibration is substituent sensitive and difficult to distinguish from the ring in-plane deformation [22]. In ortho disubstitution the ring breathing mode has three frequency intervals according to whether both substituents are heavy, or one of them is heavy while the other is light, or both of them are light. In the first case the interval is 1100–1130 cm^{-1} , in the second case 1020–1070 cm^{-1} , while in the third case it is between 630 and 780 cm^{-1} [30]. In the present case the PED analysis gives ring breathing modes at 978 cm^{-1} for PhI, 1084 cm^{-1} for PhII and 990 cm^{-1} for PhIII, as expected [22]. Raj et al. [31] reported the ring breathing mode of poly substituted benzene at 1025 cm^{-1} in IR, 1027 cm^{-1} in Raman and 1032 cm^{-1} theoretically. For ortho substituted phenyl ring the ring breathing mode is reported at 1041 cm^{-1} [32] and at 1086, 1011 cm^{-1} (theoretically) [33] and at 1020 cm^{-1} (theoretically) [34]. The C–H deformation modes of the

phenyl ring, in-plane and out-of-plane modes are expected above and below 1000 cm^{-1} respectively [22]. For the title compound, the in-plane CH deformation modes are assigned at 1121 (Raman) for PhI, 1292, 1158, 1050 (Raman) for PhII and 1181, 1127, 1020 (IR), 1174, 1021 cm^{-1} (Raman) for PhIII. The DFT calculations give these modes in the ranges 1206–1122 cm^{-1} for PhI, 1290–1055 cm^{-1} for PhII and 1310–1018 cm^{-1} for PhIII, as expected [22]. The out-of-plane C–H modes are assigned at 895 (IR), 892 (Raman), 893, 885 (DFT) for PhI, 1005, 872 (IR), 1002, 874, 773 (Raman), 1007, 965, 870, 773 (DFT) for PhII and 850 (IR), 942, 853 (Raman), 995, 947, 962, 852, 749 cm^{-1} (DFT) for PhIII. The ring substituent deformation modes are also identified and assigned (Table 2) and most of the modes are not pure but contains significant contributions from other modes also. Inorder to investigate the performance of vibrational wavenumbers of the title compound, the root mean square value between the calculated and observed wavenumbers were calculated and the RMS errors are 3.12 for IR and 3.29 for Raman modes (without considering the NH stretching mode).

4.2. Natural bond orbital analysis

In NBO analysis, a large stabilization energy E(2) value shows an

Table 3

Second-order perturbation theory analysis of Fock matrix in NBO basis corresponding to the intramolecular bonds of the title compound.

Donor(i)	Type	ED/e	Acceptor(j)	Type	ED/e	E(2) ^a	E(j)-E(i) ^b	F(i,j) ^c
S1–C33	σ	1.97343	N3–C5	σ*	0.02753	5.15	1.09	0.067
–	–	–	N4–C15	σ*	0.09003	3.66	1.05	0.056
O2–C15	π	1.99367	O2–C15	π*	0.32981	1.05	0.37	0.019
–	–	–	C5–C14	π*	0.42100	4.51	0.40	0.042
N3–C33	σ	1.98682	N3–C5	σ*	0.02753	1.80	1.38	0.045
–	–	–	N4–C16	σ*	0.03136	2.26	1.22	0.047
–	–	–	N4–C33	σ*	0.05934	1.60	1.35	0.042
–	–	–	C5–C6	σ*	0.02485	2.26	1.48	0.052
–	π	1.87937	N3–C33	π*	0.35171	1.70	0.34	0.023
–	–	–	C5–C14	σ*	0.03841	15.76	0.37	0.074
N4–C15	σ	1.98078	S1–C33	σ*	0.06401	3.19	0.96	0.050
–	–	–	N4–C16	σ*	0.03136	1.26	1.13	0.034
–	–	–	N4–C33	σ*	0.05934	2.48	1.25	0.050
–	–	–	C12–C14	σ*	0.02198	1.80	1.39	0.045
N4–C33	σ	1.98690	O2–C15	σ*	0.00906	2.32	1.44	0.052
–	–	–	N3–C33	σ*	0.01537	1.60	1.46	0.043
–	–	–	N4–C15	σ*	0.09003	1.58	1.28	0.041
–	–	–	N4–C16	σ*	0.03136	1.73	1.16	0.040
C5–C6	σ	1.97510	N3–C5	σ*	0.02753	1.65	1.17	0.039
–	–	–	N3–C33	σ*	0.01537	2.40	1.31	0.050
–	–	–	C5–C14	σ*	0.03841	4.08	1.28	0.065
–	–	–	C6–C8	σ*	0.01415	2.57	1.30	0.052
–	–	–	C14–C15	σ*	0.05967	2.92	1.18	0.053
C5–C14	σ	1.97215	O2–C15	σ*	0.05967	2.64	1.30	0.052
–	–	–	N3–C5	σ*	0.05967	1.28	1.18	0.035
–	–	–	C5–C6	σ*	0.02485	3.82	1.28	0.062
–	–	–	C12–C14	σ*	0.02198	4.36	1.29	0.067
–	–	–	C14–C15	σ*	0.05967	1.93	1.19	0.043
C14–C15	σ	1.97396	O2–C15	σ*	0.00906	1.36	1.27	0.037
–	–	–	N4–C16	σ*	0.03136	3.31	0.99	0.051
–	–	–	C5–C6	σ*	0.02485	3.05	1.25	0.055
–	–	–	C5–C14	σ*	0.03841	2.72	1.27	0.053
–	–	–	C10–C12	σ*	0.03841	1.99	1.29	0.045
–	–	–	C12–C14	σ*	0.02198	2.40	1.26	0.049
C16–C19	σ	1.97268	C22–C31	σ*	0.02331	2.47	0.65	0.039
C37–O38	π	1.99033	C37–O38	π*	0.28224	1.12	0.38	0.020
C37–N39	σ	1.98668	S1–C34	σ*	0.01537	1.54	0.97	0.034
–	–	–	N39–C40	σ*	0.03238	1.73	1.24	0.042
C40–C41	σ	1.97181	N39–C40	σ*	0.03238	1.01	1.12	0.030
–	–	–	C40–C42	σ*	0.02780	3.85	1.29	0.063
–	–	–	C41–C45	σ*	0.02610	2.63	1.29	0.052
–	–	–	C45–O59	σ*	0.02670	4.12	1.08	0.059
–	–	–	C40–C41	σ*	0.02783	3.85	1.29	0.063
–	–	–	C42–C46	σ*	0.02598	2.63	1.29	0.052
–	–	–	C46–O54	σ*	0.02671	4.12	1.08	0.059
C41–C45	σ	1.97256	N39–C40	σ*	0.03238	4.31	1.12	0.062
–	–	–	C40–C41	σ*	0.02783	2.93	1.29	0.055
–	–	–	C45–C47	σ*	0.04625	3.46	1.28	0.060
–	–	–	C47–O49	σ*	0.02450	3.80	1.08	0.057
–	–	–	O59–C60	σ*	0.01010	1.41	0.98	0.033
–	–	–	C40–C42	π*	0.02780	21.79	0.29	0.072
–	–	–	C46–C47	π*	0.39624	19.84	0.29	0.069
C42–C46	σ	1.97250	N39–C40	σ*	0.03238	4.31	1.12	0.062
–	–	–	C40–C42	σ*	0.02780	2.93	1.29	0.055
–	–	–	C46–C47	σ*	0.04625	3.46	1.28	0.060
–	–	–	C47–O49	σ*	0.02450	3.80	1.08	0.057
–	–	–	O54–C55	σ*	0.01011	3.80	1.08	0.057
C45–C47	σ	1.97627	C41–C45	σ*	0.02610	3.44	1.31	0.060
–	–	–	C46–C47	σ*	0.04625	3.38	1.29	0.059
–	–	–	C46–O54	σ*	0.02671	3.63	1.09	0.056
C46–C47	σ	1.97628	C42–C46	σ*	0.02598	3.44	1.31	0.060
–	–	–	C45–C47	σ*	0.02598	3.38	1.29	0.059
–	–	–	C45–O59	σ*	0.02598	3.63	1.09	0.056

Table 3 (continued)

Donor(i)	Type	ED/e	Acceptor(j)	Type	ED/e	E(2) ^a	E(j)-E(i) ^b	F(i,j) ^c
LPS1	σ	1.98337	N3-C33	σ^*	0.01537	2.78	1.25	0.053
—	π	1.98337	N3-C33	π^*	0.35171	21.59	0.25	0.069
LPO2	σ	1.97668	N4-C15	σ^*	0.09003	1.58	1.10	0.038
—	—	—	C14-C15	σ^*	0.05967	2.64	1.15	0.050
—	π	1.97668	N4-C15	σ^*	0.09003	28.12	0.67	0.124
—	—	—	C14-C15	σ^*	0.05967	17.45	0.72	0.102
LPN3	σ	1.97668	S1-C33	σ^*	0.06401	4.16	0.49	0.041
—	—	—	N4-C33	σ^*	0.05934	16.33	0.77	0.101
—	—	—	C5-C6	σ^*	0.02485	1.49	0.91	0.034
—	—	—	C5-C14	σ^*	0.03841	8.71	0.92	0.081
LPN4	σ	1.58809	O2-C15	π^*	0.32981	54.56	0.28	0.112
—	—	—	N3-C33	π^*	0.35171	55.07	0.27	0.110
—	—	—	C16-C19	σ^*	0.02253	5.58	0.64	0.059
LPO38	σ	1.97472	C34-C37	σ^*	0.06367	2.55	1.06	0.047
—	—	—	C37-N39	σ^*	0.07460	1.33	1.15	0.035
—	π	1.86415	S1-C33	σ^*	0.06401	1.73	0.40	0.024
—	—	—	C34-C37	σ^*	0.06367	20.29	0.63	0.103
—	—	—	C37-N39	σ^*	0.07460	25.09	0.72	0.122
LPN39	σ	1.72310	C37-O38	π^*	0.28224	67.39	0.27	0.122
—	—	—	C40-C41	σ^*	0.02783	6.62	0.84	0.071
—	—	—	C40-C42	σ^*	0.02780	6.62	0.84	0.071
LPO49	σ	1.93978	C46-C47	π^*	0.39624	6.32	0.58	0.060
—	π	1.93519	C45-C47	σ^*	0.04625	7.53	0.87	0.073
—	—	—	C46-C47	σ^*	0.04625	7.42	0.87	0.072
LPO54	σ	1.95095	C46-C47	σ^*	0.04625	7.22	1.03	0.077
—	—	—	C46-C47	π^*	0.39624	2.15	0.49	0.032
—	π	1.91374	C42-C46	σ^*	0.02598	4.82	0.96	0.062
—	—	—	C46-C47	σ^*	0.04625	1.41	0.95	0.033
—	—	—	C46-C47	π^*	0.39624	8.88	0.41	0.058
LPO59	σ	1.95096	C41-C45	σ^*	0.02610	2.05	0.49	0.031
—	—	—	C45-C47	σ^*	0.04625	7.20	1.03	0.077
—	π	1.91374	C41-C45	σ^*	0.02610	4.86	0.96	0.062
—	—	—	C41-C45	π^*	0.37415	8.94	0.41	0.058
—	—	—	C45-C47	σ^*	0.04625	1.42	0.95	0.033

^a E(2) means energy of hyper-conjugative interactions (stabilization energy in kJ/mol).^b Energy difference (a.u) between donor and acceptor i and j NBO orbitals.^c F(i,j) is the Fock matrix elements (a.u) between i and j NBO orbitals.

intensive interaction between electron-donors and electron-acceptors and the possible intensive interactions are given in Table 3. The second-order perturbation theory analysis of Fock-matrix in NBO basis shows strong intra-molecular hyper conjugative interactions are formed by orbital overlap between n(O), n(N), n(S) and $\sigma^*(C-N)$, $\pi^*(C-N)$, $\sigma^*(C-C)$, $\pi^*(C-C)$, $\pi^*(C-O)$ bond orbitals which result in intra-molecular charge transfer causing stabilization of the system.

The important hyper-conjugative interactions are: N₃-C₃₃ from S₁ of n₂(S₁) $\rightarrow\pi^*(N_3-C_{33})$, N₄-C₁₅ from O₂ of n₂(O₂) $\rightarrow\sigma^*(N_4-C_{15})$, N₄-C₃₃ from N₃ of n₁(N₃) $\rightarrow\sigma^*(N_4-C_{33})$, N₃-C₃₃ from N₄ of n₁(N₄) $\rightarrow\pi^*(N_3-C_{33})$, C₃₇-N₃₉ from O₃₈ of n₂(O₃₈) $\rightarrow\sigma^*(C_{37}-N_{39})$, C₃₇-O₃₈ from N₃₉ of n₁(N₃₉) $\rightarrow\pi^*(C_{37}-O_{38})$, C₄₆-C₄₇ from O₄₉ of n₂(O₄₉) $\rightarrow\sigma^*(C_{46}-C_{47})$, C₄₆-C₄₇ from O₅₄ of n₂(O₅₄) $\rightarrow\pi^*(C_{46}-C_{47})$, O₅₉ of n₂(O₅₉) $\rightarrow\pi^*(C_{41}-C_{45})$ with electron densities, 0.35171, 0.09003, 0.05934, 0.35171, 0.07460, 0.28224, 0.04625, 0.39624e, 0.37415e and stabilization energies, 21.59, 28.12, 16.33, 55.07, 25.09, 67.39, 7.42, 8.88, 8.94 kJ/mol. The natural hybrid orbitals with higher energy orbital and considerable p-characters and low occupations numbers are: n₂(S₁), n₂(O₂), n₂(O₃₈), n₂(O₄₉), n₂(O₅₄), n₂(O₅₉) with energies, -0.24547, -0.24101, -0.24295, -0.30641, -0.38355, -0.38346a.u. and p-characters, 99.99, 99.99, 99.85, 100, 86.50%, 86.59% and low occupation numbers, 1.84721, 1.86231,

1.86415, 1.93519, 1.91374, 1.91374. The lower energy orbitals are, n₁(S₁), n₁(O₂), n₁(O₃₈), n₁(O₄₉), n₁(O₅₄), n₁(O₅₉) with lower energies, -0.63930, -0.67242, -0.67181, -0.56242, -0.46983, -0.46997a.u. and p-characters, 28.92, 40.92, 51.02, 57.86, 72.01, 71.89% and high occupation numbers, 1.98337, 1.97668, 1.97472, 1.93978, 1.95095, 1.95096.

Thus, a very close to pure p-type lone pair orbital participates in the electron donation to the n₂(S₁) $\rightarrow\pi^*(N_3-C_{33})$, n₂(O₂) $\rightarrow\sigma^*(N_4-C_{15})$, n₁(N₃) $\rightarrow\sigma^*(N_4-C_{33})$, n₁(N₄) $\rightarrow\pi^*(N_3-C_{33})$, n₂(O₃₈) $\rightarrow\sigma^*(C_{37}-N_{39})$, n₁(N₃₉) $\rightarrow\pi^*(C_{37}-O_{38})$, n₂(O₄₉) $\rightarrow\sigma^*(C_{46}-C_{47})$, n₂(O₅₄) $\rightarrow\pi^*(C_{46}-C_{47})$ and n₂(O₅₉) $\rightarrow\pi^*(C_{41}-C_{45})$ interactions in the compound. The results are tabulated in Table 4.

4.3. Molecular electrostatic potential (MEP)

Molecular electrostatic potential (MEP) generally present in the space around the molecule by the charge distribution is very useful in understanding the sites of electrophilic and nucleophilic reaction for the study of biological recognition process and hydrogen bonding interactions. The electrostatic potential is also well suited for analyzing processes based on the recognition of one molecule by another, as in drug-receptor, and enzyme-substrate interactions, because it is through their potentials that the two species first see

Table 4

NBO results showing the formation of Lewis and non-Lewis orbitals.

Bond(A-B)	ED/e ^a	EDA%	EDB%	NBO	s%	p%
σS1-C33	1.97343	44.97	55.03	0.6706(sp ^{5.92})S+	14.35	85.65
–	-0.61816	–	–	0.7418(sp ^{2.50})C	28.53	71.47
πO2-C15	1.98232	69.94	30.06	0.8363(sp ^{1.00})O+	0.00	100.0
–	-0.35803	–	–	0.5483(sp ^{1.00})C	0.00	100.0
σN3-C33	1.97269	59.30	40.70	0.7701(sp ^{1.50})N+	39.87	60.13
–	-0.77565	–	–	0.6379(sp ^{1.67})C	37.42	62.58
πN3-C33	1.98682	61.69	38.31	0.7855(sp ^{1.00})N+	0.00	100.0
–	-0.90925	–	–	0.6189(sp ^{1.00})C	0.00	100.0
σN4-C15	1.98078	64.20	35.80	0.8012(sp ^{1.97})N+	33.70	66.30
–	-0.80959	–	–	0.5984(sp ^{2.38})C	29.56	70.44
σN4-C33	1.98690	37.20	62.80	0.6099(sp ^{1.88})N+	34.69	65.31
–	-0.84791	–	–	0.7925(sp ^{1.93})C	34.04	65.96
σC5-C6	1.97510	48.85	51.15	0.6989(sp ^{1.78})C+	36.02	63.98
–	-0.69569	–	–	0.7152(sp ^{1.93})C	34.09	65.91
σC5-C14	1.97215	49.29	50.71	0.7021(sp ^{1.80})C+	35.67	64.33
–	-0.70636	–	–	0.7121(sp ^{1.94})C	33.99	66.01
σC14-C15	1.97396	51.70	48.30	0.7190(sp ^{2.26})C+	30.64	69.36
–	-0.67720	–	–	0.6950(sp ^{1.63})C	38.06	61.94
σC16-C19	1.97268	50.45	49.55	0.7103(sp ^{2.53})C+	28.33	71.67
–	-0.59509	–	–	0.7039(sp ^{2.94})C	25.39	74.61
πC37-O38	1.99033	30.20	69.80	0.5495(sp ^{1.00})C+	0.00	100.0
–	-0.35969	–	–	0.8355(sp ^{1.00})O	0.00	100.0
σC37-N39	1.98668	37.38	62.62	0.6114(sp ^{2.15})C+	31.75	68.25
–	-0.83783	–	–	0.7913(sp ^{1.69})N	37.17	62.83
σC40-C41	1.97181	50.44	49.56	0.7102(sp ^{1.74})C+	36.45	63.55
–	-0.71495	–	–	0.7040(sp ^{1.84})C	35.23	64.77
σC40-C42	1.97181	50.44	49.56	0.7102(sp ^{1.74})C+	36.45	63.55
–	-0.71494	–	–	0.7040(sp ^{1.84})C	35.23	64.77
σC41-C45	1.97256	50.05	49.95	0.7074(sp ^{1.90})C+	34.52	65.48
–	-0.71671	–	–	0.7068(sp ^{1.63})C	37.99	62.01
σC42-C46	1.97250	50.04	49.96	0.7074(sp ^{1.90})C+	34.52	65.48
–	-0.71668	–	–	0.7068(sp ^{1.63})C	37.99	62.01
σC45-C47	1.97627	49.81	50.19	0.7057(sp ^{1.72})C+	36.78	63.22
–	-0.72734	–	–	0.7085(sp ^{1.67})C	37.48	62.52
σC46-C47	1.97628	49.80	50.20	0.7057(sp ^{1.72})C+	36.77	63.23
–	-0.72736	–	–	0.7085(sp ^{1.67})C	37.49	62.53
n1S1	1.98337	–	–	sp ^{0.41}	71.08	28.92
–	-0.63930	–	–	–	–	–
n2S1	1.84721	–	–	sp ^{1.00}	0.01	99.99
–	-0.24547	–	–	–	–	–
n1O2	1.97668	–	–	sp ^{0.69}	59.08	40.92
–	-0.67242	–	–	–	–	–
n2O2	1.86231	–	–	sp ^{99.99}	0.01	99.99
–	-0.24101	–	–	–	–	–
n1N3	1.89048	–	–	sp ^{2.79}	26.34	73.66
–	-0.33265	–	–	–	–	–
n1N4	1.58809	–	–	sp ^{1.00}	0.00	100.0
–	-0.26520	–	–	–	–	–
n1O38	1.97472	–	–	sp ^{0.69}	58.98	51.02
–	-0.67181	–	–	–	–	–
n2O38	1.86415	–	–	sp ^{99.99}	0.15	99.85
–	-0.24295	–	–	–	–	–
n1N39	1.72310	–	–	sp ^{1.00}	0.00	100.0
–	-0.25904	–	–	–	–	–
n1O49	1.93978	–	–	sp ^{1.37}	42.14	57.86
–	-0.56242	–	–	–	–	–
n2O49	1.93519	–	–	sp ^{1.00}	0.00	100.0
–	-0.30641	–	–	–	–	–
n1O54	1.95095	–	–	sp ^{2.57}	27.99	72.01
–	-0.46983	–	–	–	–	–
n2O54	1.91374	–	–	sp ^{6.40}	13.50	86.50
–	-0.38355	–	–	–	–	–
n1O59	1.95096	–	–	sp ^{2.57}	28.01	71.89
–	-0.46997	–	–	–	–	–
n2O59	1.91374	–	–	sp ^{6.41}	13.49	86.51
–	-0.38346	–	–	–	–	–

^a ED/e is expressed in a.u.

each other. To visually consider the most probable sites of the title compound for an interaction with electrophilic and nucleophilic species, MEP was calculated at the DFT/B3LYP method with 6-311++G(d,p) (5D, 7F) set from the optimized geometry. While electrophilic reactivities visualized by red color which indicate the negative regions of the molecule, the nucleophilic reactivities colored by blue, indicating the positive regions of the molecule as shown in Fig. 4. Regions of negative potential are usually associated with the lone pair of electronegative atoms. As can be seen from the MEP map of the title molecule, negative region is mainly localized over the C=O groups and the mono substituted phenyl ring which are electrophilic. The maximum positive region is localized on the NH and hydrogen atoms which are nucleophilic.

4.4. Nonlinear optical properties

The calculated first hyperpolarizability of the title compound is 2.66×10^{-30} e.s.u which is 20.46 times that of standard NLO material urea (0.13×10^{-30} e.s.u) [35]. For quinazoline derivatives the reported values of first hyperpolarizability are 2.75×10^{-30} e.s.u [36] and 5.05×10^{-30} e.s.u [37]. The molecular second hyperpolarizability value can aid in gaining information about the physical properties of materials to understand the origin of third harmonic signals generated in chemical and biological structures. Such knowledge is effective in the development of optical devices including the application of optical communication, optical switching, signal processing and optical computing [38]. The average second hyperpolarizability has been calculated by using the following expression.

$$\gamma_{av} = 1/5 [\gamma_{xxxx} + \gamma_{yyyy} + \gamma_{zzzz} + 2\gamma_{xxyy} + 2\gamma_{xxzz} + 2\gamma_{yyzz}]$$

The amount of charge transfer for the molecule depends on the nature of the end group of the molecule. Increase of π -conjugated chain length in organic molecules, in general, enhances the magnitude of hyperpolarizability. The calculated value of γ_{av} for the title compound is -56.009×10^{-37} esu. Thus the present investigation provides a new route to design high performance NLO materials.

4.5. Frontier molecular orbital analysis

HOMO-LUMO band gap plays a very crucial role in determining the chemical reactivity, stability of the molecule, UV–Vis spectra, chemical reactions, electrical and optical properties. LUMO energy means the ability to accept an electron while HOMO energy means ability to donate an electron. The conjugated molecules are characterized by a highest occupied molecular orbital-lowest unoccupied molecular orbital gap (HOMO-LUMO), which is the result of a significant degree of intermolecular charge transfer from the end capping electron-donor groups to the efficient electron-acceptor groups through a pi-conjugated path. The strong charge transfer interaction through pi-conjugated bridge results in substantial groundstate donor-acceptor mixing the appearance of a charge transfer band in the electronic spectrum. Therefore, an electron density transfers occurs from the more aromatic part of the pi-conjugated system in the electron-donor side to its electron-withdrawing part. The energy gap between the HOMO and LUMO is a critical parameter in determining molecular electrical transport properties and for predicting the most reactive position in pi-electron systems and also explains several types of reaction in conjugated system. The highest occupied molecular orbital (HOMO) and the lowest unoccupied molecular orbital (LUMO) of the title compound are shown in Fig. 5). HOMO is localized over the mono-substituted phenyl ring, ortho-substituted phenyl ring, the

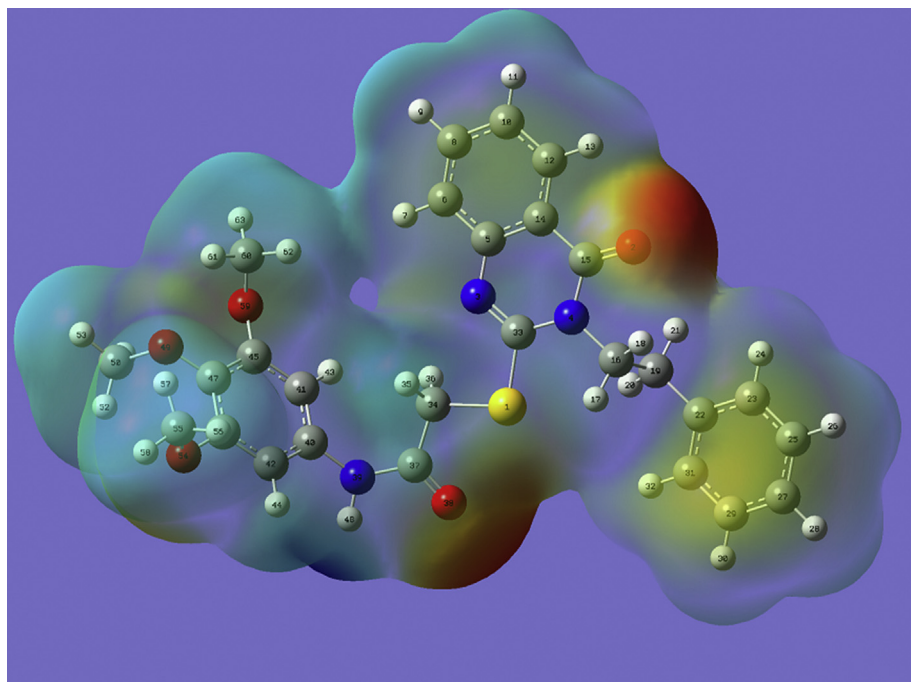


Fig. 4. MEP plot of 2-(4-oxo-3-phenethyl-3,4-dihydroquinazolin-2-ylthio)-N-(3,4,5-trimethoxyphenyl) acetamide.

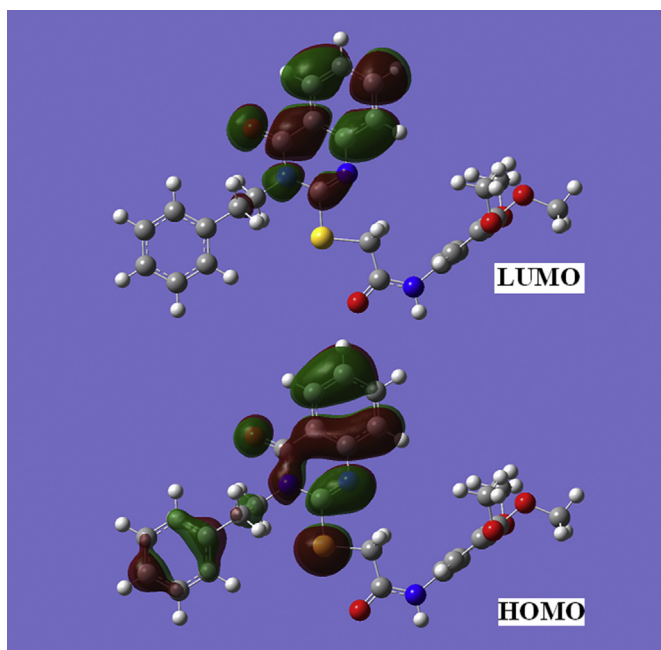


Fig. 5. HOMO-LUMO plots of 2-(4-oxo-3-phenethyl-3,4-dihydroquinazolin-2-ylthio)-N-(3,4,5-trimethoxyphenyl) acetamide.

quinazoline ring and the sulfur atom while the LUMO is localized over ortho-substituted phenyl ring and quinazoline ring. Therefore a charge transfer occurs through the ring systems. For understanding various aspects of pharmacological sciences including drug design and the possible eco-toxicological characteristics of the drug molecules, several new chemical reactivity descriptors have been proposed. Using HOMO and LUMO orbital energies, the ionization energy and electron affinity can be expressed as: $I = -E_{\text{HOMO}}$, $A = -E_{\text{LUMO}}$ [39]. The hardness η and chemical potential μ are given

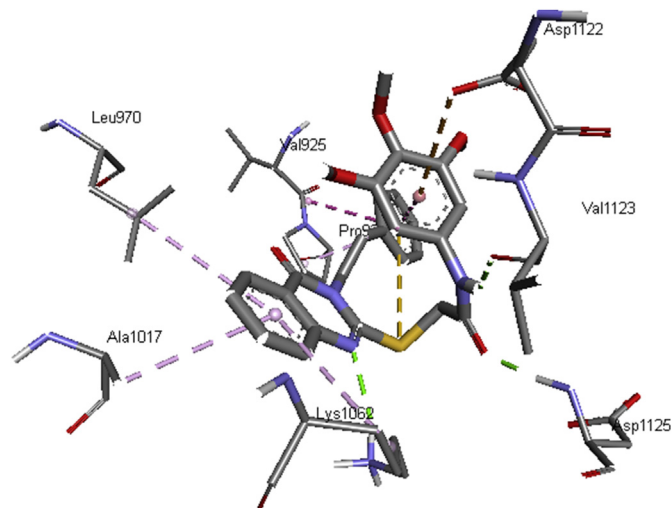


Fig. 6. Schematic for the docked conformation of active site of title compound at BRCA2 complex.

the following relations $\eta = (I - A)/2$ and $\mu = -(I + A)/2$, where I and A are the first ionization potential and electron affinity of the chemical species [40]. For the title compound, $E_{\text{HOMO}} = -8.539$ eV, $E_{\text{LUMO}} = -2.327$ eV, Energy gap = HOMO-LUMO = 6.212 eV, Ionization potential $I = 8.539$ eV, Electron affinity $A = 2.327$ eV, global hardness $\eta = 3.106$ eV, chemical potential $\mu = -5.433$ eV, global electrophilicity $= \mu^2/2\eta = 4.752$ eV. It is seen that the chemical potential of the title compound is negative and it means that the compound is stable.

4.6. Molecular docking

Quinazoline are a large class of active chemical compounds possess a wide variety of biological activities such as anti HIV,

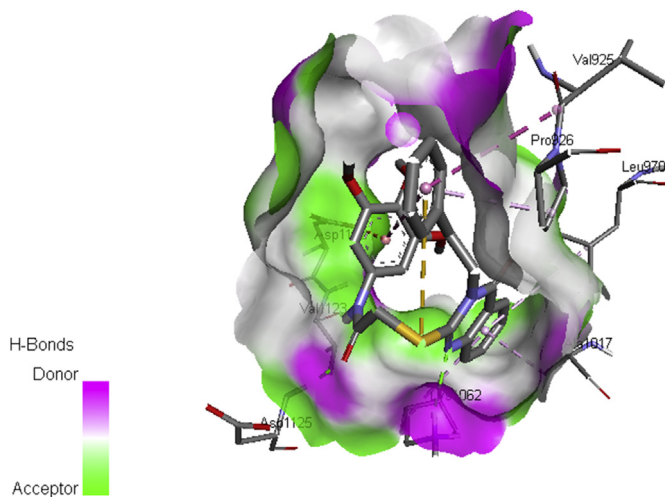


Fig. 7. The docked protocol reproduced the co-crystallized conformation with H-bond (green), π -alkyl (pink) and π -anion (brown).

Table 5

The binding affinity values of different poses of the title compound predicted by AutodockVina.

Mode	Affinity (kcal/mol)	Distance from best mode (Å)	
	—	RMSD l.b.	RMSD u.b.
1	−7.6	0.000	0.000
2	−7.5	2.639	5.713
3	−7.4	3.828	7.711
4	−7.3	2.319	4.846
5	−7.3	2.881	5.062
6	−7.3	2.330	4.964
7	−7.3	2.804	4.694
8	−7.2	3.640	6.122
9	−7.2	1.962	5.952

anticancer [41,42], antifungal, antibacterial, anti-mutagenic, anti-convulsant etc. [43]. High resolution crystal structure of BRCA2 complex was downloaded from the protein data bank website (PDB ID: 3EU7). All molecular docking calculations were performed on Auto Dock Vina software [44]. The protein was prepared for docking by removing the co-crystallized ligands, waters and co-factors. The Auto Dock Tools (ADT) graphical user interface was used to calculate Kollman charges and polar hydrogen's. The ligand was prepared for docking by minimizing its energy at B3LYP/6-311++G(d,p) (5D, 7F) level of theory. Partial charges were calculated by Geistenger method. The active site of the enzyme was defined to include residues of the active site within the grid size of $40 \text{ \AA} \times 40 \text{ \AA} \times 40 \text{ \AA}$. The most popular algorithm, Lamarckian Genetic Algorithm (LGA) available in Autodock was employed for docking. The docking protocol was tested by extracting co-crystallized inhibitor from the protein and then docking the same. The docking protocol predicted the same conformation as was present in the crystal structure with RMSD value well within the reliable range of 2 \AA [45]. Amongst the docked conformations, one which binded well the active site was analyzed for detailed interactions in Discover Studio Visualizer 4.0 software. The ligand binds at the active site of the substrate (Figs. 6 and 7) by weak non-covalent interactions. Lys1062, Asp1125 and Val1123 amino acid forms H-bond with pyrimidine ring, C=O and N–H group respectively. Leu970, Ala1017 and Lys1062 form π -alkyl interaction with phenyl ring. Asp1122 amino acid forms electrostatic interaction

(π -anion) with phenyl ring. The docked ligand title compound forms a stable complex with BRCA2 complex and gives a binding affinity (ΔG in kcal/mol) value of -7.6 (Table 5). These preliminary results suggest that the compound might exhibit inhibitory activity against BRCA2 complex.

4.7. Geometrical parameters

In the title compound, the C–S bond lengths are 1.7853 and 1.8304 \AA while the reported values are in the range 1.7675 – 1.8641 \AA [46] and 1.7710 – 1.8110 \AA [31]. The shortening of the bond length of C_{15} – O_2 (1.2205 \AA) and C_{37} – O_{38} (1.2192 \AA) could be assigned a double bond character. The C–O bond lengths of the title compound are C_{46} – $O_{54} = 1.3715 \text{ \AA}$, C_{55} – $O_{54} = 1.4372 \text{ \AA}$, C_{47} – $O_{49} = 1.3740 \text{ \AA}$, C_{50} – $O_{49} = 1.4391 \text{ \AA}$, C_{45} – $O_{59} = 1.3701 \text{ \AA}$ and C_{60} – $O_{59} = 1.4367 \text{ \AA}$ and all the C–O bond lengths are greater than the average distance of 1.362 \AA found among phenols [47] and the increase is due to the noticeable intra-molecular hydrogen bonding experienced by the molecule [48]. The bond lengths of C_{40} – N_{39} (1.4215 \AA), C_{37} – N_{39} (1.3759 \AA), C_{15} – N_4 (1.4157 \AA), C_{33} – N_4 (1.3859 \AA), and C_5 – N_{39} (1.3825 \AA) are shorter than the normal C–N bond length of about 1.48 \AA and this point into the effect of resonance in this part of the molecule [49]. All the carbon–carbon bond lengths in the benzene rings lie in the range 1.3919 – 1.4045 \AA for PhI, 1.3832 – 1.4088 \AA for PhII and 1.3936 – 1.3996 \AA for PhII and bond lengths are somewhere in between the normal values for a single (1.54 \AA) and a double bond (1.33 \AA) [50]. The acetamide group is tilted from the phenyl ring PhI according to the torsion angles, C_{45} – C_{41} – C_{40} – $N_{39} = 178.4^\circ$, C_{41} – C_{40} – N_{39} – $C_{37} = 51.9^\circ$, C_{46} – C_{42} – C_{40} – $N_{39} = -177.3^\circ$ and C_{42} – C_{40} – N_{39} – $C_{37} = -130.2^\circ$. The quinazoline moiety is planar with respect to the phenyl ring PhII, as is evident from the torsion angles C_{12} – C_{14} – C_{15} – $N_{43} = 179.4^\circ$, C_{12} – C_{14} – C_5 – $N_3 = 180.0^\circ$, C_6 – C_5 – N_3 – $C_{33} = 179.8^\circ$ and C_6 – C_5 – C_{14} – $C_{15} = -179.4^\circ$ and the CH_2 groups at C_{19} and C_{16} are tilted from the phenyl ring PhIII, as is evident from the torsion angles, C_{25} – C_{23} – C_{22} – $C_{19} = 178.4^\circ$, C_{23} – C_{22} – C_{19} – $C_{16} = -88.0^\circ$, C_{29} – C_{31} – C_{22} – $C_{19} = -178.4^\circ$ and C_{31} – C_{22} – C_{19} – $C_{16} = 90.3^\circ$. At N_4 position, the bond angles C_{33} – N_4 – C_{15} is increased by 1.0° , C_{33} – N_4 – C_{16} is increased by 2.6° and C_{15} – N_4 – C_{16} is decreased by 3.7° from 120° and this is due to the interaction between O_2 and the methylene at C_{16} position. At C_{22} position, the bond angles are C_{31} – C_{22} – $C_{23} = 118.6^\circ$, C_{31} – C_{22} – $C_{19} = 120.8^\circ$ and C_{23} – C_{22} – $C_{19} = 120.7^\circ$ and the reduction in the angle C_{31} – C_{22} – C_{23} is due to presence of adjacent methylene groups. At C_{15} position, the bond angles, N_4 – C_{15} – C_{14} is decreased by 5.6° and C_{14} – C_{15} – O_2 is increased by 5.0° from 120° and this variation is due to the interaction between O_2 and the adjacent methylene groups. Similarly at C_5 position, the bond angles C_6 – C_5 – $C_{14} = 118.9^\circ$, N_3 – C_5 – $C_6 = 119.1^\circ$ and C_{14} – C_5 – $N_3 = 122.0^\circ$ and this asymmetry in angles is due to the interaction between the quinazoline and PhII rings. Also at C_{33} position, the bond angles N_3 – C_{33} – $N_4 = 124.8^\circ$ and N_4 – C_{33} – $S_1 = 115.3^\circ$ and this asymmetry in angles is due to the interaction between the quinazoline ring and adjacent moieties. Similarly at N_{39} position, the bond angles C_{40} – N_{39} – $C_{37} = 130.9^\circ$, C_{40} – N_{39} – $H_{48} = 116.6^\circ$ and C_{37} – N_{39} – $H_{48} = 119.9^\circ$ and this asymmetry in angles is due to the interaction between the NH group and the oxygen atom O_{38} and at C_{37} position, the bond angle N_{39} – C_{37} – C_{34} is reduced by 2.6 and C_{34} – C_{37} – O_{38} is increased by 2.2 from 120° , which shows the hydrogen bonding between O_{38} and H_{48} .

5. Conclusion

The experimental and theoretical vibrational spectra of 2-(4-oxo-3-phenethyl-3,4-dihydroquinolin-2-ylthio)-N-(3,4,5-

trimethoxyphenyl) acetamide were investigated. The complete assignments were performed on the basis of potential energy distribution of the vibrational modes. The stimulated FT-IR and Raman spectra of the title compound show good agreement with the observed spectra. The calculated HOMO and LUMO energies show that charge transfer occur within the molecule. The calculated first hyperpolarizability of the title compound is 20.46 times that of standard NLO material urea and hence the title compound and its derivatives are good object for further studies in nonlinear optics. Molecular docking study shows that the ligand binds at the active site of the substrate by weak non-covalent interactions; Lys1062, Asp1125 and Val1123 amino acid forms H-bond with pyrimidine ring, C=O and N–H group respectively; Leu970, Ala1017 and Lys1062 form π -alkyl interaction with phenyl ring; Asp1122 amino acid forms electrostatic interaction (π -anion) with phenyl ring.

Acknowledgments

The authors extend their appreciation to the Deanship of Scientific Research at King Saud University for funding the work through the research group project No. RGP-VPP-163.

References

- [1] K.M. Kimberm, L. Yonno, R. Hearlip, B. Weichman, *Agent Actions* 39 (1993) C77.
- [2] A.J. Duplantier, J.B. Cheng, *Annu. Rep. Med. Chem.* 29 (1994) 73.
- [3] E.A. Sener, K.K. Bingol, I. Oren, O.T. Arpacı, I. Yalcın, N. Altanlar, *Farmaco* 55 (2000) 469.
- [4] V. Alagarsamy, R. Giridhar, H.R. Yadav, R. Revathi, K. Rukmani, E. De Clercq, *Indian J. Pharm. Sci.* 68 (2006) 532.
- [5] V.K. Srivastava, A. Singh, A. Gucati, K. Shankar, *Indian J. Chem.* 26 (1987) 652.
- [6] D.P. Gupta, S. Ahmed, A. Kumar, K. Shankar, *Indian J. Chem.* 27 (1988) 1060.
- [7] V. Joshi, R.P. Chaurasia, *Indian J. Chem.* 26 (1987) 602.
- [8] I.R. Prouse (Ed.), *Drugs Future*, vol. 18, 1993, p. 475.
- [9] S.V. Bhandari, B.J. Deshmame, S.T. Gore, V.T. Raparti, C.V. Khachane, A.P. Sarkate, *Pharmacologyonline* 2 (2008) 604.
- [10] A.A. Bekhit, N.S. Habib, A. Bekhit, *Boll. Chim. Farm* 140 (2001) 297.
- [11] M.R. Azza, E.R. Eman, G.E. Fatma, *Arch. Pharm.* 337 (2004) 527.
- [12] V.K. Pandey, D. Mishra, S. Sukla, *Indian Drugs* 31 (1994) 532.
- [13] V.K. Pandey, *Indian Drugs* 26 (1988) 168.
- [14] V.K. Pandey, M. Gupta, D. Mishra, *Indian Drugs* 33 (1996) 409.
- [15] A.K. Sengupta, A.A. Gupta, J. Antibact. Antifung. Agent 8 (1980) 7.
- [16] M.J. Frisch, G.W. Trucks, H.B. Schlegel, G.E. Scuseria, M.A. Robb, J.R. Cheeseman, G. Scalmani, V. Barone, B. Mennucci, G.A. Petersson, H. Nakatsuji, M. Caricato, X. Li, H.P. Hratchian, A.F. Izmaylov, J. Bloino, G. Zheng, J.L. Sonnenberg, M. Hada, M. Ehara, K. Toyota, R. Fukuda, J. Hasegawa, M. Ishida, T. Nakajima, Y. Honda, O. Kitao, H. Nakai, T. Vreven, J.A. Montgomery Jr., J.E. Peralta, F. Ogliaro, M. Bearpark, J.J. Heyd, E. Brothers, K.N. Kudin, V.N. Staroverov, T. Keith, R. Kobayashi, J. Normand, K. Raghavachari, A. Rendell, J.C. Burant, S.S. Iyengar, J. Tomasi, M. Cossi, N. Rega, J.M. Millam, M. Klene, J.E. Knox, J.B. Cross, V. Bakken, C. Adamo, J. Jaramillo, R. Gomperts, R.E. Stratmann, O. Yazyev, A.J. Austin, R. Cammi, C. Pomelli, J.W. Ochterski, R.L. Martin, K. Morokuma, V.G. Zakrzewski, G.A. Voth, P. Salvador, J.J. Dannenberg, S. Dapprich, A.D. Daniels, O. Farkas, J.B. Foresman, J.V. Ortiz, J. Cioslowski, D.J. Fox, *Gaussian 09, Revision D.01, Gaussian, Inc, Wallingford CT*, 2013.
- [17] A. Irfan, R. Jin, A.G. Al-Sehem, A.M. Asiri, *Spectrochim. Acta* 110 (2013) 60.
- [18] A. Irfan, A.G. Al-Sehem, M.S. Al-Assiri, *J. Fluor. Chem.* 157 (2014) 52.
- [19] J.B. Foresman, in: E. Frisch (Ed.), *Exploring Chemistry with Electronic Structure Methods: a Guide to Using Gaussian*, Gaussian Inc., Pittsburg, PA, 1996.
- [20] R. Dennington, T. Keith, J. Millam, *GaussView, Version 5, Semichem Inc, Shawnee Mission KS*, 2009.
- [21] J.M.L. Martin, C. Van Alsenoy, *GAR2PED, A Program to Obtain a Potential Energy Distribution from a Gaussian Archive Record*, University of Antwerp, Belgium, 2007.
- [22] N.P.G. Roeges, *A Guide to the Complete Interpretation of IR Spectra of Organic Compounds*, Wiley, New York, 1994.
- [23] N.B. Colthup, L.H. Daly, S.E. Wiberly, *Introduction to IR and Raman Spectroscopy*, Academic Press, New York, 1990.
- [24] R.M. Silverstein, F.X. Webster, *Spectrometric Identification of Organic Compounds*, sixth ed., John Wiley, Asia, 2003.
- [25] B. Smith, *Infrared Spectral Interpretation, A Systematic Approach*, CRC Press, Washington DC, 1999.
- [26] L.J. Bellamy, *The IR Spectra of Complex Molecules*, John Wiley and Sons, New York, 1975.
- [27] Y.S. Mary, C.Y. Panicker, H.T. Varghese, K. Raju, T.E. Bolelli, I. Yildiz, M.C. Granadeiro, H.I.S. Nogueira, *J. Mol. Struct.* 994 (2011) 223.
- [28] G. Louran, M. Lapkowski, S. Quillard, A. Pron, J.B. Buisson, S. Lefrant, *J. Phys. Chem.* 100 (1996) 6998.
- [29] H.T. Varghese, C.Y. Panicker, D. Philip, P. Pazdera, *Spectrochim. Acta* 67 (2007) 1055.
- [30] G. Varsanyi, *Assignments of Vibrational Spectra of Seven Hundred Benzene Derivatives*, Wiley, New York, 1974.
- [31] A. Raj, Y.S. Mary, C.Y. Panicker, H.T. Varghese, K. Raju, *Spectrochim. Acta* 113 (2013) 28.
- [32] A. Chandran, H.T. Varghese, C.Y. Panicker, C. VanAlsenoy, G. Rajendran, *J. Mol. Struct.* 1001 (2012) 29.
- [33] C.Y. Panicker, H.T. Varghese, K.R. Ambujakshan, S. Mathew, S. Ganguli, A.K. Nanda, V. Van Alsenoy, Y.S. Mary, *Eur. J. Chem.* 1 (2010) 37.
- [34] C.Y. Panicker, H.T. Varghese, K.R. Ambujakshan, S. Mathew, S. Ganguli, A.K. Nanda, C. Van Alsenoy, Y.S. Mary, *J. Mol. Struct.* 963 (2010) 137.
- [35] C. Adant, C. Dupuis, J.L. Bredas, *Int. J. Quantum. Chem.* 56 (1995) 497.
- [36] S.H.R. Sebastian, A.M.S. Al-Tamimi, N.R. El-Brolosy, A.A. El-Emam, C.Y. Panicker, C. Van Alsenoy, *Spectrochim. Acta* 134 (2015) 316.
- [37] C.Y. Panicker, H.T. Varghese, K.R. Ambujakshan, S. Mathew, S. Ganguli, A.K. Nanda, C. Van Alsenoy, Y.S. Mary, *J. Mol. Struct.* 963 (2010) 137.
- [38] D. Tokarz, R. Cisek, N. Prent, U. Fekl, V. Barzda, *Anal. Chim. Acta* 755 (2012) 86.
- [39] A.G. Al-Sehem, A. Irfan, *Arab. J. Chem.* DOI:10.1016/j.arabjc.2013.06.019.
- [40] R.G. Parr, R.G. Pearson, *J. Am. Chem. Soc.* 105 (1983) 7512.
- [41] A.M.M. El-Saghier, E.A. Ahmed, A.M.A. Mahmoud, *J. Pharm. Appl. Chem.* 1 (2015) 9.
- [42] D.K. Dodiya, S.J. Vaghasia, A.R. Trivedi, H.K. Ram, V.H. Shah, *Indian J. Chem.* 49 (2010) 802.
- [43] R. Rajput, A.P. Mishra, *Int. J. Pharm. PharmSci.* 4 (2012) 66.
- [44] O. Trott, A.J. Olson, *J. Comput. Chem.* 31 (2010) 455.
- [45] B. Kramer, M. Rarey, T. Lengauer, *Proteins Struct. Funct. Genet.* 37 (1999) 228.
- [46] Y.S. Mary, K. Raju, I. Yildiz, O. Temiz-Arpaci, H.I.S. Nogueira, C.M. Granadeiro, C. Van Alsenoy, *Spectrochim. Acta* 96 (2012) 617.
- [47] F.H. Allen, O. Kennard, D.G. Watson, L. Brammer, A.C. Orpen, R. Taylor, *J. Chem. Soc. Perkin Trans. 2* (1987) S01.
- [48] Y.S. Mary, C.Y. Panicker, T.S. Yamuna, M.S. Siddegowda, H.S. Yathirajan, A.A. Al-Saadi, C. Van Alsenoy, *Spectrochim. Acta* 132 (2014) 491.
- [49] R.T. Ulahannan, C.Y. Panicker, H.T. Varghese, R. Musiol, J. Jampilek, C. Van Alsenoy, J.A. War, A.A. Al-Saadi, *Spectrochim. Acta* 151 (2015) 335.
- [50] Y.S. Mary, P.J. Jojo, C. Van Alsenoy, M. Kaur, M.S. Siddegowda, H.S. Yathirajan, H.I.S. Nogueira, S.M.A. Cruz, *Spectrochim. Acta* 120 (2014) 340.